



# **Geophysical Research Letters**

### RESEARCH LETTER

10.1029/2020GL090521

#### **Key Points:**

- Mid-Atlantic margin backstripping residuals reflecting nonthermal changes in land elevation can be represented by a sinusoidal geometric form with a ~1,000 km wavelength
- The spatial shift in apparent backstripping residuals through time is consistent with rates of motion for the North American plate
- A wave of relative uplift that influences the Mid-Atlantic margin since 35 Ma appears to be superimposed on a signal of longterm subsidence

#### **Supporting Information:**

- Supporting Information S1
- · Supporting Information S2
- Figure S1
- Table S1
- Table S2
- · Data Set S1
- Movie S1

## Correspondence to:

W. J. Schmelz, wjs107@eps.rutgers.edu

#### Citation:

Schmelz, W. J., Miller, K. G., Kopp, R. E., Mountain, G. S., & Browning, J. V. (2021). Influence of mantle dynamic topographical variations on US Mid-Atlantic continental margin estimates of sea-level change. *Geophysical Research Letters*, 48, e2020GL090521. https://doi.org/10.1029/2020GL090521

Received 26 AUG 2020 Accepted 7 JAN 2021

© 2021. American Geophysical Union. All Rights Reserved.

## Influence of Mantle Dynamic Topographical Variations on US Mid-Atlantic Continental Margin Estimates of Sea-Level Change

William J. Schmelz<sup>1,2</sup>, Kenneth G. Miller<sup>1,2</sup>, Robert E. Kopp<sup>1,2</sup>, Gregory S. Mountain<sup>1,2</sup>, and James V. Browning<sup>1,2</sup>

<sup>1</sup>Department of Earth and Planetary Sciences, Rutgers University, Piscataway, NJ, USA, <sup>2</sup>Institute of Earth, Ocean, and Atmospheric Sciences, Rutgers University, New Brunswick, NJ, USA

**Abstract** Spatial analysis of discrepancies in sea-level estimates derived from "backstripping" Mid-Atlantic margin cores reveals a coherent signal that can be fit with a  $10^3$  km wavelength, 45 m amplitude sinusoid that moved across the margin at a rate and direction of motion generally opposite to that of the North American Plate. This signal we observe suggests topographical uplift occurred over much of the Mid-Atlantic region since 35 Ma and may be superimposed upon a longer-wavelength signal of Cenozoic subsidence associated with the subducted Farallon plate passing beneath the Mid-Atlantic margin. Our statistical modeling of Mid-Atlantic margin strata suggests that: (a) Cenozoic subsidence is likely to have occurred, but is very unlikely to have exceeded 100 m in magnitude; and (b) variations in ocean basin volume are likely to have contributed to  $39 \pm 24$  m  $(1\sigma)$  of global-mean geocentric sea-level fall over the past 55 million years.

**Plain Language Summary** Knowledge of sea-level variations in the geological past help constrain predictions of sea-level rise due to future warming. One of the ways to measure prehistoric sealevel change is to study preserved marine sediments that record changes in water depth. These analyses are complicated by the history of these sediments since their burial, including the sinking (subsidence) or uplift of the region and specific locations examined. Some effects of sediment burial and subsidence can be accounted for through modeling, including the effects of sediment compaction, loading due to sediment mass, and cooling of the crust. However, changes in elevation caused by the passage of lateral heterogeneities in the mantle beneath the study area, often called the effects of mantle dynamic topography (MDT), are difficult to detect. We used statistical modeling techniques to reveal the influence of changes in MDT on the preserved sediments of the Mid-Atlantic continental margin. Our results show that this process affected estimates of sea-level generated from these sediments, though to a lesser extent than some model studies predicted.

#### 1. Introduction

Through backstripping, the stratigraphy of the passive, tectonically quiescent Mid-Atlantic margin has helped define our understanding of Cenozoic global-mean geocentric sea-level (GMGSL; Gregory et al., 2019) variations (Kominz et al., 2016, 2008; Miller et al., 1998, 2005, 2011, 2020a; Van Sickel et al., 2004). Backstripping is a method that progressively removes the effects of compaction with burial of sediments, isostatic/ flexural loading of the lithosphere, and the thermal subsidence of the passive margin (Bond et al., 1989; Watts & Steckler, 1979) to provide a record of GMGSL plus any nonthermal source of relative sea-level (RSL) changes that are not explicitly accounted for (Bond et al., 1989; Kominz et al., 2008). Therefore, the extent to which estimates of sea-level change derived from these analyses (Kominz et al., 2008; Miller et al., 2005, 2020a) reflect GMGSL change hinges on whether a sizable fraction of Mid-Atlantic Cenozoic RSL is attributable to sources of nonthermal subsidence or uplift that are not accounted for by backstripping, such as mantle dynamic topography (MDT), glacial isostatic adjustment, faulting, folding, or flexural loading effects that deviate from the form of thermal subsidence through time (see Kominz et al., 2016).

Agreement of the backstripping residuals from many different sites across the margin gives confidence that there is a shared GMGSL signal (Kominz et al., 2008; Miller et al., 2005), but cannot separate that signal from regionally pervasive nonthermal vertical land motion. Mantle convection models predict Late

SCHMELZ ET AL. 1 of 11



Cretaceous-Cenozoic topographical variations due to MDT (Flament et al., 2013; Gurnis, 1992; Mitrovica et al., 1989; Spasojevic & Gurnis, 2012) associated with the subducted Farallon plate that could imprint the backstripping results with regional effects (Moucha et al., 2008; Müller et al., 2008; Spasojević et al., 2008). However, models of MDT vary considerably in their estimates of the magnitude and sign of Cenozoic topographical motion for the Mid-Atlantic margin (Liu, 2015); for example, Moucha et al. (2008) predicted Cenozoic uplift, while Müller et al. (2008) and Spasojević et al. (2008) predicted subsidence. Additionally, sea-level estimates that account exclusively for the fraction of GMGSL change associated with changes in ocean basin volume (e.g., Müller et al., 2008; Wright et al., 2020) better fit the backstripping data if the margin has undergone Cenozoic subsidence (Muller et al., 2008). However, uncertainty for estimates of the fraction of GMGSL change driven by changes in the ocean basin shape is relatively large (>100 m at 66 Ma; Wright et al., 2020).

Here, we compare backstripping residuals derived from the stratigraphy of the Mid-Atlantic margin to a new estimate of Cenozoic barystatic sea-level change (changes in GMSL due to variations in land water and ice storage) derived from benthic foraminiferal  $\delta^{18}$ O coupled with Mg/Ca paleotemperature estimates (Miller et al., 2020a), and a new estimate of sea-level change driven by changes in ocean basin volume (Wright et al., 2020). We fit these sea-level estimates and their uncertainties using a Bayesian hierarchical model that can be decomposed to isolate components of the GMGSL and RSL signals within the backstripping residuals in order to estimate the likely partial contributions of: (a) MDT toward Cenozoic RSL change on the Mid-Atlantic margin; and (b) changes in ocean-basin shape toward Cenozoic GMGSL. We then test whether the spatial structure of the derived MDT signal matches predictions of topographical variations from MDT through space and time.

## 2. Terminology

We adopt the sea-level terminology of Gregory et al. (2019), expanding on it to account for factors that are relevant on geological timescales.

RSL change  $\Delta R$  is defined as the change in the time-mean of sea surface height (SSH) relative to the sea floor. Thus, RSL change is the sum of the change in the sea-surface height,  $\Delta \eta$ , and the negative change in the sea-floor height,  $-\Delta F$ .

Global-mean sea-level (GMSL) change h is defined as the increase in the volume of the ocean  $\Delta V$  divided by the area of the ocean  $A_0$ , which is for the purposes of this definition treated as fixed, and is thus equal to the global mean of  $\Delta R$  (Equation 1).

$$h \, 1 \, \Delta V \, / \, A_0 \tag{1}$$

Global-mean geocentric sea-level (GMGSL) change h', by contrast, is measured relative to a reference ellipsoid. As noted by Gregory et al. (2019), GMSL is unaffected by a uniform change in the height of the sea floor, whereas GMGSL is not; thus  $\Delta V$  in the definition of GMSL is augmented by the change in the volume of the ocean basin,  $\Delta L$ . We define GMGSL to include the effects of a changing ocean area (Equation 2).

$$h' 1 \frac{\Delta V \tilde{Z} \Delta L}{A_0 \tilde{Z} \Delta A} \quad "h \quad \frac{\Delta L}{A_0} - \frac{V}{\Delta A}$$
 (2)

Thus, GMGSL can be viewed as GMSL augmented by terms reflecting change in mean sea-floor height and decremented by terms reflecting increases in ocean area. (Note that  $\frac{\Delta L}{A0}$  is equal to the average of  $\Delta F$  over the ocean area; this is why GMSL is equal to the global mean of  $\Delta R$  if  $\Delta A=0$ .) We relate these ocean-basin volume contributors (OBVSL;  $h_{\rm OB}$ ) to GMGSL in Equation 3.

$$h_{OB} 1 h' - h \tag{3}$$

GMSL change is the sum of barystatic sea-level change (BSL;  $h_b$ ) and global-mean thermosteric sea-level change ( $h_\theta$ ). Changes in sea-surface height that differ from GMSL change arise from ocean dynamic

SCHMELZ ET AL. 2 of 11



sea-level change ( $\zeta$ ) and from changes in the geoid (G') driven by the gravitational and rotational effects of mass redistribution in the oceans, cryosphere, and lithosphere (Equation 4).

$$\Delta \setminus 1 \ h' \ \check{Z}\Delta G' \ \check{A} \ n$$
 (4)

Changes in the sea-floor height are driven by factors including compaction with burial of sediments ( $\Delta F_C$ ), isostatic/flexural loading of the lithosphere ( $\Delta F_{\rm FLEX}$ ), the thermal subsidence ( $\Delta F_{\rm TH}$ ) of the passive margin, MDT ( $\Delta F_{\rm MDT}$ ), the deformational component of glacial isostatic adjustment ( $\Delta F_{\rm GIA}$ ), and tectonics ( $\Delta F_{\rm TECT}$ ). The stratigraphy of continental margin sediments reflects all of the processes that contribute to  $\Delta R$  (Equation 5).

Backstripping progressively removes  $\Delta F_C$ ,  $\Delta F_{\rm FLEX}$  and  $\Delta F_{\rm TH}$  (Bond et al., 1989; Watts & Steckler, 1979), leaving residuals (*r*SL; Equation 6) that comprise GMGSL change plus any source of RSL change that is not accounted for in backstripping (Bond et al., 1989; Kominz et al., 2008).

$$r$$
SL 1  $h_b$   $\check{Z}h_e$   $\check{Z}_{OB}$   $\Delta \check{Z}_{C}$ t $\check{Z}$   $\Delta n$  ! $\Delta F_{MDT}$ !  $\Delta F_{GIA}$ !  $\Delta F_{TECT}$  (6)

In general, we neglect  $h_\theta$ ,  $\Delta G^{\dagger}$  and  $\Delta \zeta$  as being small relative to the errors in inferring RSL from stratigraphy (Figure S1a).

### 3. Data

We use three datasets in our analyses. The first is a collection of backstripping derived sea-level estimates (rSL) from stratigraphic data collected at 18 sites on the Mid-Atlantic margin. We divide these estimates of rSL into three subsets of data. The first consists of estimates derived from 14 sites located onshore in New Jersey and just offshore (Browning et al., 2006; Kominz et al., 2008; Miller et al., 2005). The second comprises the backstripping estimates from three coreholes collected 43–65 km offshore NJ during IODP Expedition 313 (Kominz et al., 2016; Mountain et al., 2010). The third is the Bethany Beach, Delaware backstripping record (Browning et al., 2006). These three subsets are defined as the onshore, offshore, and southern datasets, respectively (Figure 1).

The second data set is the  $\delta^{18}O_{benthic}$ -Mg/Ca BSL proxy derived from a new, Pacific benthic foraminiferal  $\delta^{18}O$  splice (Miller et al., 2020a) and Pacific Mg/Ca paleotemperature estimates (Cramer et al., 2011). These  $\delta^{18}O$  data were used to capture the ice-volume component of BSL change. A benthic foraminiferal paleotemperature equation (Lynch-Stieglitz et al., 1999) and the Mg/Ca-based paleotemperature estimates allowed for the estimation of changes in  $\delta^{18}O$  of seawater ( $\delta^{18}O_{seawater}$ ). A conversion factor (0.13‰/10 m; Winnick & Caves, 2015) was used to relate  $\delta^{18}O_{seawater}$  to a sea-level component of ice-volume change. These estimates are largely representative of GMSL change on a geological time scale, as changes in thermosteric effects and lakes and groundwater storage are smaller in scale (~10 m amplitude) than changes in ice-volume (~200 m amplitude; Miller et al., 2020b). These data have an estimated error of ~10–20 m (Cramer et al., 2011; Miller et al., 2020a; Raymo et al., 2018).

Finally, we use a data set that estimates change in OBVSL (Wright et al., 2020). These data represent likely sea-level change from the changing volume of ocean basins attributable to processes such as variations in the rate of production of ocean crust or of emplacement of large igneous provinces, and variations in sedimentation through time. These estimates of OBVSL change and their uncertainty combined with the Miller et al. (2020a)  $\delta^{18}$ O<sub>benthic</sub>-Mg/Ca BSL proxy represent an estimate of GMGSL change and its error. A notable limitation of the Wright et al. (2020) data set is that it does not include contributions from the influence of global-mean dynamic topography on OBVSL. Other studies indicate that this process could contribute 90 m (Conrad & Husson, 2009) to ~140–190 m (Spasojevic & Gurnis, 2012) of Cenozoic OBVSL rise. A contribution of this magnitude would eliminate the estimated 117 m of Cenozoic OBVSL fall predicted by Wright et al. (2020), or even alter its sign. This possibility is accounted for in our statistical model that relies exclusively on the BSL proxy to represent GMGSL change.

SCHMELZ ET AL. 3 of 11

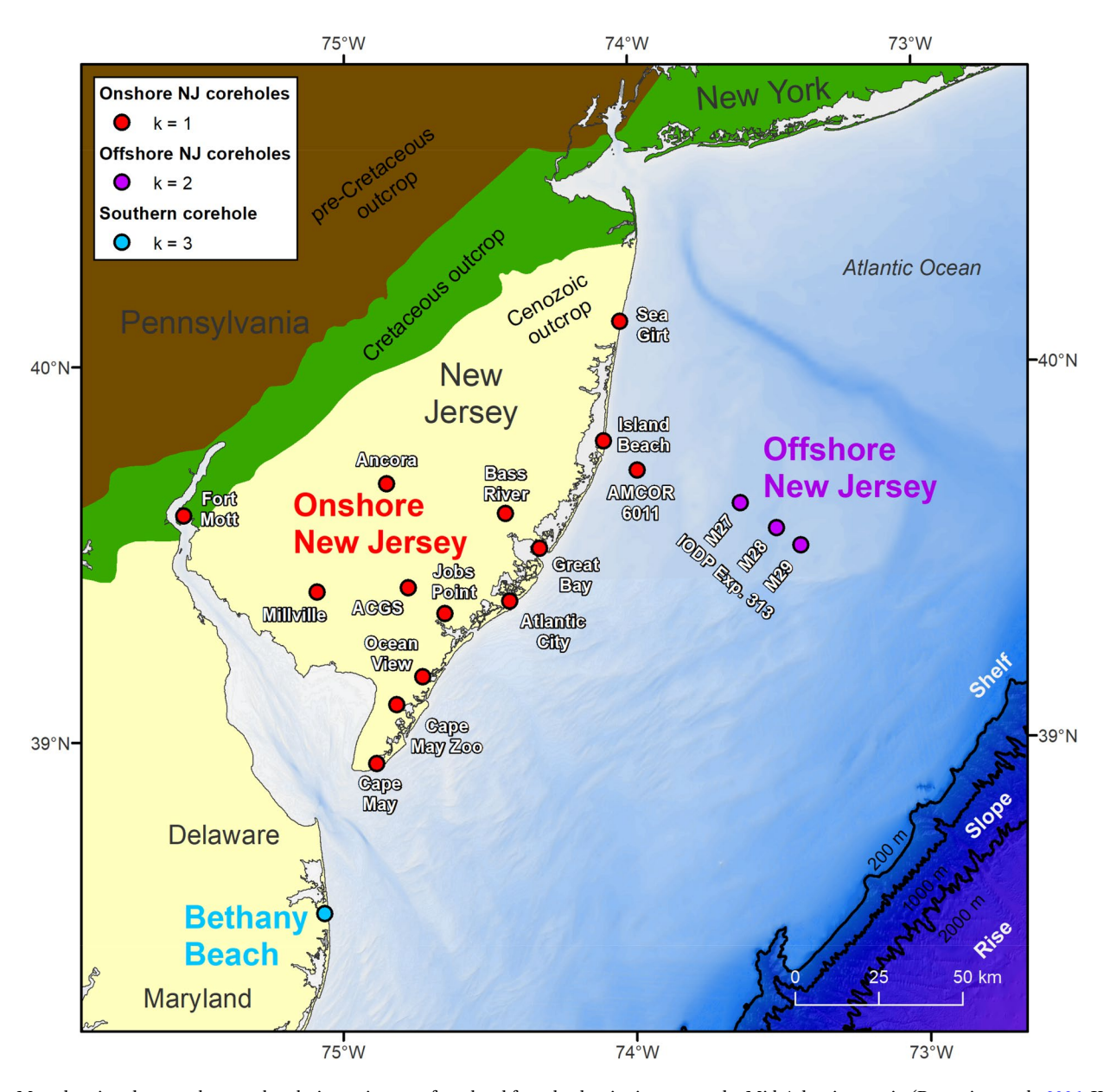


**Figure 1.** Map showing the core data used to derive estimates of sea level from backstripping across the Mid-Atlantic margin (Browning et al., 2006; Kominz et al., 2016, 2008; Miller et al., 2005). The backstripping results have been divided into three geographical locations comprised of: (a) the onshore New Jersey sites; (b) the offshore New Jersey sites; and (c) a single southern site at Bethany Beach, DE.

#### 4. Methods

## 4.1. Methods for Statistically Modeling Sea Level to Extract Backstripping Residuals.

We applied a Bayesian hierarchical model with Gaussian process priors (Ashe et al., 2019; Rasmussen & Williams, 2006) to estimate the change in rSL, BSL, and OBVSL as these processes are represented by data. The structure of the statistical model reflects the presence of the BSL and OBVSL signals in both the proxy datasets and the backstripping data, while also capturing the regional/local sea-level signals present in the backstripping data. This allows us to assess the geometric structure of the statistically modeled estimates of differences between the spatially distinct subsets of the backstripping data and GMGSL, as well as the variation/motion of these differences through space and time.

The hierarchical model has three levels: (a) a data level that represents the sea-level measurements and their uncertainties; (b) a process level that represents the distribution of sea-level values through time as a

SCHMELZ ET AL. 4 of 11



Gaussian process prior; and (c) a hyperparameter level that captures the distribution of parameter values controlling the structure of the statistical model (see supporting information Text S1).

At the data level, the  $\delta^{18}$ O<sub>benthic</sub>-Mg/Ca BSL proxy,  $x_i$  (Equation 7), represents the sum of the estimate of BSL change through time,  $h_b(t)$ , and the error associated with those data. That error is the sum of  $Y_i^x$ , associated with the nominal error assigned to the  $\delta^{18}$ O<sub>benthic</sub>-Mg/Ca BSL proxy data, and  $w_{h_bj}$ , which captures any additional error. The Wright et al. (2020) data,  $y_i$  (Equation 8), represent OBVSL change. Its error,  $Y_i^y$ , was digitized from Wright et al. (2020). The backstripping data,  $z_i$  (Equation 9), represent the backstripped sea-level estimate, rSL $_{k,j}(t)$ , from a given time, t, and space, t, plus the error associated with each data point, or the sum of  $Y_i^x$  and  $w_{rSL_j}$  t. The spatial marker, t, identifies data from the onshore, offshore, and southern subareas with values of 1, 2, and 3, respectively.

$$x_i \perp h_b \uparrow \downarrow_i \quad \{ \check{Z} Y_i^x \quad \check{W}_{hb} \quad t$$
 (7)

$$y_i + 1 h_{OB} \int_{i}^{t} \left\{ \check{Z} V_i^{V} \right\}$$
 (8)

$$z_i \perp rSL_k f |_{t_i} \quad \stackrel{\wedge}{\mathbb{Z}} \mathcal{V}_i^{\varepsilon} \quad \stackrel{\wedge}{\mathbb{Z}}_{rSI} \quad t_i f$$
 (9)

At the process level, estimates of sea-level,  $h_b(t)$  (Equation 10),  $h_{OB}(t)$  (Equation 11), http:// (Equation 12), and  $rSL_k(t)$  (Equation 13), are represented as a combination of component processes (Figure S1b). Considering uncertainty associated with the OBVSL data, including both the error on estimates of OBVSL components and the influence of potentially offsetting processes like global-mean dynamic topography that were not accounted for, we consider two alternative models. In the first model, the "static ocean basin" model, OBVSL is assumed to be constant and does not contribute to GMGSL change (http://Equation 12). In the "growing ocean basin" model (Equation 12), we allow OBVSL to vary.

$$h_b f \nmid \underline{h} m t f |\underline{b}_b \nmid t \underline{d} f |$$
 (10)

$$h_{OB} = h \cdot n \cdot t \int \mathcal{D}_{OB} t \cdot \mathcal{D}_{OB}$$
 (11)

$$rSL_k$$
 f\rangle \frac{1}{2} \hfrac{1}{2} \

The component processes are each modeled with a zero-mean Gaussian process prior and are structured to capture discrete physical processes operating on different timescales. Nonlinear component process, m(t), and temporally linear term,  $l_b(t)$ , are inferred to represent a BSL signal driven by changes in ice-volume. The constant term,  $c_b$ , serves as an offset for  $h_b(t)$ . These components contribute to GMGSL change and are shared with rSL in both the static and growing ocean basin models. The OBVSL process  $h_{OB}(t)$  is also represented by a nonlinear, a temporally linear, and an offset component. These components  $(n(t), l_{OB}(t), and c_{OB}, respectively)$  contribute to GMGSL change and are shared with rSL $_k(t)$  exclusively in the growing ocean basin model.

The temporally linear term  $l_k(t)$  is unique to  $rSL_k(t)$ , and is inferred to represent long-term trends in the measurement of rSL change. This linear term represents the long-term differences between the individual backstripped estimates of rSL change and change in GMGSL. Additional long-term variations among the spatially distinct backstripping sea-level estimates are captured by the nonlinear process  $\Delta_k(t)$ . The term  $E_k(t)$  captures high-amplitude variations correlated at relatively short time-scales (<400 kyr) that are likely distinct from the differences captured by slowly varying linear and  $\Delta$  functions. The constant term,  $c_k$ , captures the difference in time-average sea-level between each backstripping record and GMGSL. Therefore,

SCHMELZ ET AL. 5 of 11



 $r\mathrm{SL}_k(t)$ , or the sum of: (a)  $h^{\dagger\dagger}$ ; (b) linear terms  $l_k(t)$  and  $c_k$ ; and (c) the nonlinear terms  $\Delta_k(t)$  and  $E_k(t)$ , represents a location specific sea-level estimate comprised of GMGSL plus the effect of regional processes that affect RSL change at the backstripping locations, such as but not limited to MDT. Estimates of  $h_b(t)$ ,  $h^{\dagger\dagger}$ , and  $r\mathrm{SL}_k(t)$  are portrayed in Figure 2.

## 4.2. Methods for Isolating Continental Margin Processes Within the Statistically Modeled Backstripping Residuals.

Global and regional sea-level change occurs due to a number of physical processes that change the volume of water in the ocean or change the volume of ocean basins (Miller et al., 2005) that act on different timescales and distinctively in space. For example, changes in BSL and GMTSL can act on relatively short (decadal- $10^5$  year) timescales, whereas variations in ocean crust production and sedimentation (components of OBVSL) take much longer ( $10^6$ – $10^8$  years) to substantially affect GMGSL (Miller et al., 2020b). Regional/local subsidence processes can be instantaneous for a process like a single faulting event, rapid for GIA ( $\sim$ 5 kyr scale), or act on long ( $10^6$ – $10^7$  year) timescales like mantle driven processes (Petersen et al., 2010). GMGSL processes will affect RSL at all locations relatively (though not exactly) equivalently, whereas sea-level changes specific to a given region only affect RSL at a specific location at a given time.

We use the spatial and temporal characteristics of the physical processes that contribute to the differences between the backstripping estimates and GMGSL to isolate and extract a signal potentially attributable to mantle driven processes. We eliminate the variations that are not related to mantle processes by removing signals that are global in nature, or are correlated on timescales shorter than 2 Myr (" $\tau$ " values in Table S1). These constraints eliminate the GMGSL signal, h'(t), and the ' $E_k(t)$ ' functions (high-frequency, regional/local variations). This leaves the spatially varying long-term components unique to  $rSL_k(t)$ , including  $\Delta_k(t)$  and  $l_k(t)$ , and the offset,  $c_k$ . These components represent the differences between rSL change at each subarea and GMGSL (Figures 2d and 2h) that vary at the time-scales mantle process affect regional topography (e.g., Petersen et al., 2010). If a signal from MDT exists within these data, then these curves of long-term rSL components minus GMGSL should contain it.

## 4.3. Methods for Modeling the Backstripping Residuals through Space and Time

We calculate the dimensions of a topographical form and its trajectory through the Cenozoic that fit the long-term differences between *r*SL and GMGSL change in the static ocean basin model. To do this, we used the long-term differences between the onshore, offshore, and southern spatial subsets of *r*SL and BSL (Figure 2d) to calibrate a simple dynamic topographical model. The model simulates the apparent change in topography through space and time captured by the backstripping record using a dampened sine curve with a constant form that moves at a constant rate and direction (Equations S13–S16). It oscillates once, creating a succession of subsidence-uplift-subsidence at a given location through time.

The shape and motion of the dynamic topography are fit by maximizing the likelihood that a given set of parameters simulates dynamic topography that accounts for the backstripping residuals using an MCMC sampling routine (supporting information Text S2). The optimal values and uncertainties for the parameters are listed in Table S2. The fit of the model output to the backstripping residuals and maps of the topography is presented in Figure 3 and Movie S1.

### 5. Results

## 5.1. Quantifying Differences Between rSL and Components of GMGSL

We performed two statistical analyses, one that assumed a static ocean basin and a second that included estimates of OBVSL change in GMGSL. Both analyses show that spatially distinct portions of the back-stripping record vary differentially relative to GMGSL over the past 35 Ma (cf., Figures 2d and 2h), and are indicative of a regional/local process, like MDT, acting on rSL. This is expected as there is not a large contribution of OBVSL to GMGSL (Figure 2g) since 35 Ma. However, OBVSL is likely to contribute more toward GMGSL from 66 Ma to 35 Ma (Figures 2e and 2g) and that results in differences between the two analyses.

SCHMELZ ET AL. 6 of 11

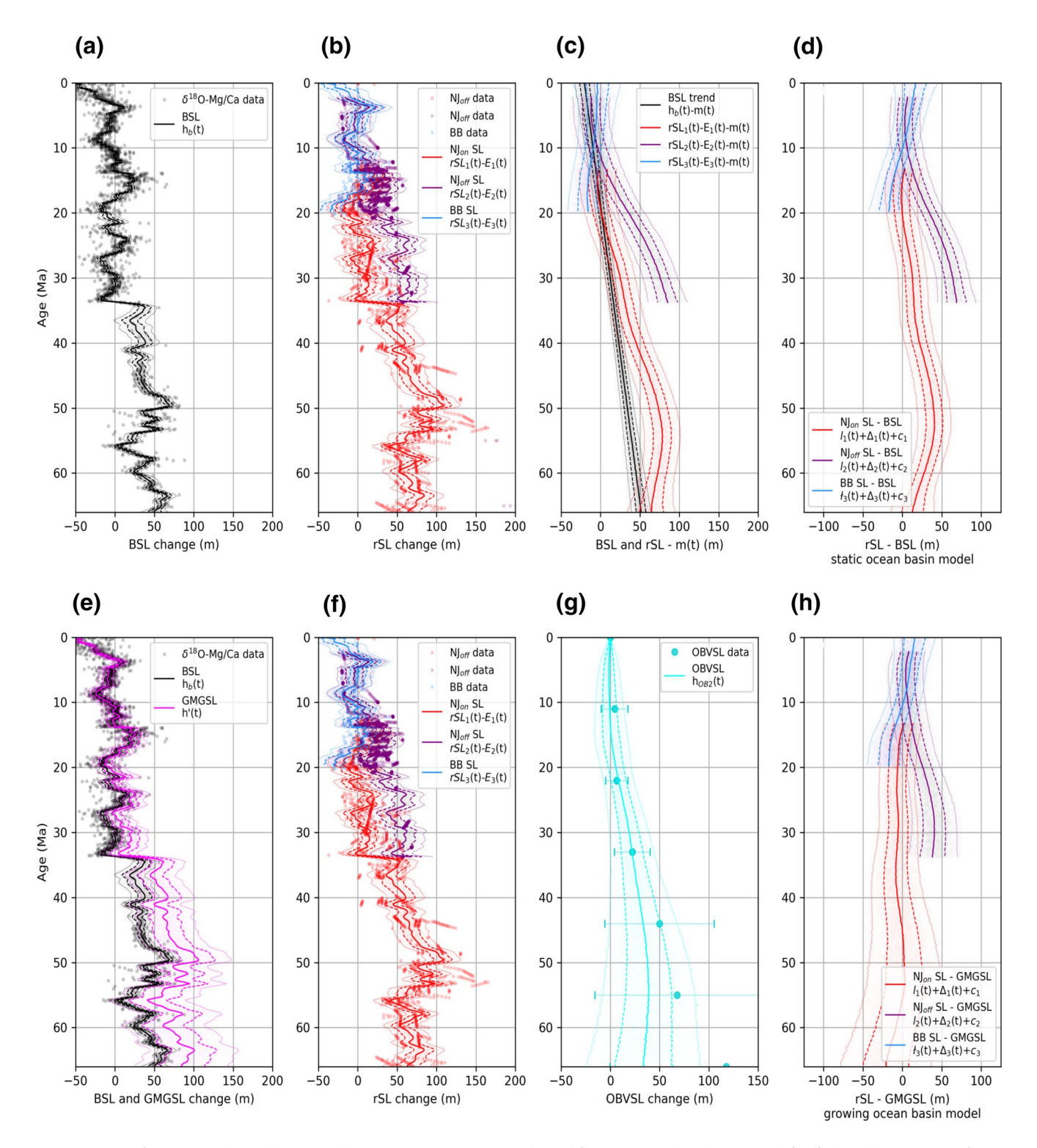


Figure 2. Estimates of GMGSL and rSL change and their component variations derived from statistical analyses. Panels (a–d) show the estimates of BSL recorded by  $\delta^{18}$ O-Mg/Ca proxy and rSL from backstripping studies of core sites on the Mid-Atlantic margin (a and b), as well as the decomposition of those estimates to isolate the long term trends associated with them (c) and the difference between the regionally grouped rSL estimates and BSL within the static ocean basin model (d). Panels (e and f) show estimates of GMGSL and rSL variations (e and f) that incorporate estimates of OBVSL (g). Panel (h) shows the difference between long-term components of rSL and GMGSL within the growing ocean basin model.

SCHMELZ ET AL. 7 of 11

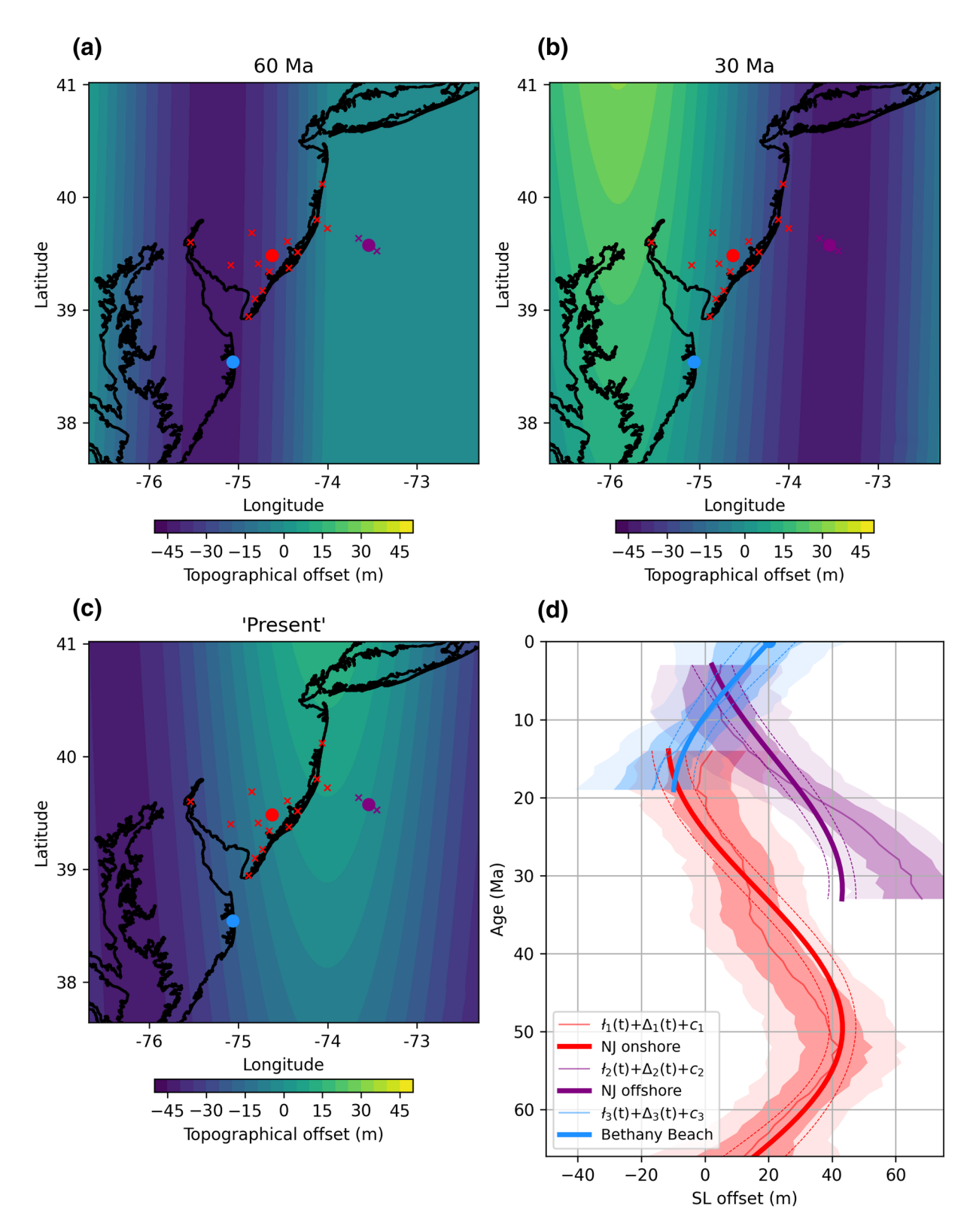


Figure 3. Estimates of dynamic topography at 60 Ma (a), 30 Ma (b), and at present (c) extracted from fitting a sine curve of constant form moving at a constant rate in a constant direction to the statistically derived, spatially segregated backstripping residuals of the Mid-Atlantic margin. The red, purple, and blue dots in the images represent the centered locations of the onshore New Jersey cores, the offshore New Jersey cores, and the Bethany Beach core, respectively. (d) Plot of the best fit modeled topography through time to the corresponding backstripping residuals at each location. The results are plotted with the uncertainties for both the backstripping residuals ( $1\sigma$  [dark shading] and  $2\sigma$  [light shading]) and the model output ( $2\sigma$  [dashed line]).

SCHMELZ ET AL. 8 of 11



Utilizing the static ocean basin model, the relative variation observed in the offshore NJ record (rSL $_2$  - BSL; Figure 2d) from 34 Ma to 3 Ma is replicated ~20 Myr earlier in the onshore record from 52 Ma to 20 Ma (rSL $_1$  - BSL; Figure 2d). These results would indicate similar rates of relative uplift in both regions over those durations, 1.3  $\pm$  0.4 m/Myr onshore and 2.1  $\pm$  0.5 m/Myr for the offshore. For comparison, these rates of change are slightly less than the topographical variations of 10–40 m/Myr modeled for the past 3 Ma on the Mid-Atlantic margin by Rowley et al. (2013). An assessment of the 3.5 Myr old Orangeburg Scarp by Moucha and Ruetenik (2017) indicate a maximum of ~40–50 m of dynamic topography generated during this time, although the amount of uplift attributable to dynamic topography varies considerably (from 0 to ~40–50 m) across its 800 km extent exemplifying the spatial heterogeneity of this process.

The growing ocean basin model shows that the difference between the onshore backstripping record and GMGSL can be explained by an increase in OBVSL contribution between 66 Ma and 20 Ma. The subducted Farallon slab might simultaneously generate a long-wavelength subsidence component of dynamic topography (Müller et al., 2008; Spasojević et al., 2008) and shorter-wavelength mantle upwelling anomalies (e.g., Conrad et al., 2004; Forte et al., 2007) that have resulted in relative topographical uplift over the majority of the Mid-Atlantic region since  $\sim$ 35 Ma (Moucha et al., 2008). Subsidence associated with the subducted slab appears to be the dominant process in this location early in the Cenozoic, and/or the large uncertainty associated with OBVSL before 35 Ma (Figure 2g) obscures shorter-wavelength mantle-upwelling driven variation within rSL relative to GMGSL. The coherence of spatially modeling the components of the static ocean basin model rSL curves (Figure 3) supports the possibility of the latter. However, without better spatial control on rSL from 66 to 35 Ma, as there is only onshore NJ data during this time, it is not possible to definitively state whether the onshore portion of rSL captures MDT or is generated largely/exclusively by variations in OBVSL.

Spasojević et al. (2008) provide modeled estimates of dynamic topography for the Mid-Atlantic margin that span the Cenozoic; they predicted at least 50 m of subsidence for the Mid-Atlantic margin since the Eocene, with a high-end estimate of 200 m. Our analysis that explicitly incorporates the Wright et al. (2020) estimates of OBVSL toward GMGSL change indicates that it is likely ( $\sim$ 77% probability), but far from certain, that Cenozoic net subsidence occurred on this margin. However, there is only a very small chance (<1%) that this subsidence was greater than 100 m, and our analysis precludes the possibility of 200 m of subsidence. This analysis also suggests that there has been 39  $\pm$  24 m (1 $\sigma$ ) of GMGSL fall attributable to the changes in OBVSL over the past 55 Myr. The 68 m OBVSL fall predicted by Wright et al. [2020] since 55 Ma is within 2 $\sigma$  error. Our probabilistic assessment of OBVSL changes would benefit from comparisons to similar studies conducted using other margins.

#### 5.2. Modeling the Spatial Distribution of rSL Differences Relative to BSL Through Time

The spatial modeling results (Figure 3) show that a sine curve moving at a constant velocity across the Mid-Atlantic margin can replicate the statistically derived differences between the spatially referenced estimates of rSL and BSL through the Cenozoic. From 66 to  $\sim$ 50 Ma the model shows a region of relative subsidence moving across the onshore NJ sites that correspond with an increase in the rSL values relative to BSL in this region (NJ<sub>on</sub> SL - BSL; Figure 2d). Our model shows relative uplift onshore from  $\sim$ 50 to 15 Ma, corresponding to a decrease in the "NJ<sub>on</sub> SL - BSL" differences, and a topographical high reaches these sites  $\sim$ 20–15 Ma. This topographical high reached the Bethany Beach site, located to the south of the onshore NJ sites, at  $\sim$ 20 Ma. In the time since, this site underwent apparent relative subsidence and the rSL values relative to BSL at Bethany Beach (BB SL - BSL; Figure 2d) have decreased. This sequence is replicated offshore with the apex of relative subsidence occurring  $\sim$ 30 Ma and the topographical high reaching these sites at the present. The "NJ<sub>off</sub> SL - BSL" differences (Figure 2d) between 35 and  $\sim$ 20 Ma were the most challenging to fit with the spatial model. The model mean barely fits within the 95% confidence interval, likely due to uncertainties in the older offshore record (e.g., Katz et al., 2013) and/or contribution from OBVSL variation.

The parameters that control the form of the topography (Table S2) reasonably fit expectations for a process like MDT. The topography has an amplitude of  $\sim$ 43 m and wavelengths of  $\sim$ 460 km in the x-dimension and  $\sim$ 4,890 km in the y-dimension. The direction and rate of motion is north-northeast,  $\sim$ 50–76 degrees counterclockwise from east, and 13.8 km/Myr (8.7–22.6 km/Myr; 16th to 84th percentile). Over the past 66 Ma, the plate tectonic data compiled Müller et al. [2019] show a spot location in New Jersey moving  $\sim$ 166°,

SCHMELZ ET AL. 9 of 11



counterclockwise from due east, along with the North American plate at an average speed of 16.8 km/Myr. The difference in directions of motion calculated by the geometric modeling and the plate tectonic model would indicate a northward component of motion for the mantle process or a component of rotation associated with the motion of the North American plate. The rates of motion between the two processes are very similar, indicating that the motion of the North American plate is likely to be the primary driver of the changes in the location we observe in the sea-level anomalies.

#### 6. Conclusion

We statistically modeled the relationship between backstripped sea-level estimates from three discrete locations across the Mid-Atlantic margin and components of GMGSL. We decomposed the statistical model to isolate local/regional components that are correlated at timescales over  $10^7$  years and are likely generated by variations in MDT. Fitting a 3-dimensional sine function that moves at a constant rate and direction captures the spatiotemporal structure of this dynamic topography that is characterized by: (a) a wavelength on the order of hundreds to thousands of km; (b) a rate of motion that is similar to the Cenozoic average rate of motion for North American plate; and (c) a direction of motion that is generally opposite to the Cenozoic direction of motion for the North American plate. This sinusoid produces a pulse of relative uplift onshore New Jersey from 50 to 20 Ma that is also observed offshore from  $\sim$ 35-3 Ma. Our statistical model accounting for OBVSL indicates that  $\sim$ 40 m of tectonically driven GMGSL fall likely occurred since 55 Ma and net Cenozoic subsidence. These observations suggest that the subducted Farallon slab generated both a long-term subsidence effect and shorter-wavelength mantle anomalies associated with the more recent relative uplift of the Mid-Atlantic margin. We conclude there is strong evidence for Cenozoic MDT influences on this margin, although the record prior to 35 Ma is still relatively uncertain.

## **Data Availability Statement**

The backstripping-derived sea-level estimates used for this research are published in these papers: (1) Browning et al. (2006); (2) Kominz et al. (2008); and (3) Kominz et al. (2016). These data have been uploaded as supporting information and will be permanently archived in the NCEI paleoclimatology database. The  $\delta^{18}O_{benthic}$ -Mg/Ca GMGSL proxy data [Miller et al., 2020a] are available for download through NCEI (https://www.ncdc.noaa.gov/paleo-search/study/29130). The estimates of sea-level variations attributable to changes in the volume of ocean basins (Wright et al., 2020) are available for download from the EarthByte repository (ftp://ftp.earthbyte.org/Data\_Collections/Wright\_etal\_2020\_ESR/).

#### Acknowledgments

The authors acknowledge the Office of Advanced Research Computing (OARC) at Rutgers University for providing access to high-performance computing resources. The code used for the analyses in this paper will be uploaded to and stored on GitHub. Supported by NSF grants OCE-1657013 (Miller) and OCE-1702587 (Kopp) and IODP/TAMRE.

#### References

- Ashe, E. L., Cahill, N., Hay, C., Khan, N. S., Kemp, A., Engelhart, S. E., et al. (2019). Statistical modeling of rates and trends in Holocene relative sea level. *Quaternary Science Reviews*, 204, 58–77.
- Bond, G. C., Kominz, M. A., Steckler, M. S., Grotzinger, J. P., & Crevello, P. (1989). Role of thermal subsidence, flexure, and eustasy in the evolution of early Paleozoic passive-margin carbonate platforms. *Controls on Carbonate Platform and Basin Development: SEPM, Special Publication*, 44, 39–61.
- Browning, J. V., Miller, K. G., McLaughlin, P. P., Kominz, M. A., Sugarman, P. J., Monteverde, D., et al. (2006). Quantification of the effects of eustasy, subsidence, and sediment supply on Miocene sequences, mid-Atlantic margin of the United States. *GSA Bulletin*, 118(5–6), 567–588.
- Conrad, C. P., & Husson, L. (2009). Influence of dynamic topography on sea level and its rate of change. Lithosphere, 1(2), 110–120.
- Conrad, C. P., Lithgow-Bertelloni, C., & Louden, K. E. (2004). Iceland, the Farallon slab, and dynamic topography of the North Atlantic. *Geology*, 32(3), 177.
- Cramer, B., Miller, K. G., Barrett, P., & Wright, J. (2011). Late Cretaceous–Neogene trends in deep ocean temperature and continental ice volume: Reconciling records of benthic foraminiferal geochemistry (δ18O and Mg/Ca) with sea level history. *Journal of Geophysical Research: Oceans*, 116(C12), C12023. 10.1029/2011JC007255
- Flament, N., Gurnis, M., & Müller, R. D. (2013). A review of observations and models of dynamic topography. *Lithosphere*, 5(2), 189–210. Forte, A. M., Mitrovica, J. X., Moucha, R., Simmons, N. A., & Grand, S. P. (2007). Descent of the ancient Farallon slab drives localized mantle flow below the New Madrid seismic zone. *Geophysical Research Letters*, 34(4), L04308. 10.1029/2006GL027895
- Gregory, J. M., Griffies, S. M., Hughes, C. W., Lowe, J. A., Church, J. A., & Fukimori, I., et al. (2019). Concepts and terminology for sea level: Mean, variability and change, both local and global. *Surveys in Geophysics*, 40(6), 1251–1289.
- Gurnis, M. (1992). Rapid continental subsidence following the initiation and evolution of subduction. Science, 255(5051), 1556-1558.
- Katz, M. E., Browning, J. V., Miller, K. G., Monteverde, D. H., Mountain, G. S., & Williams, R. H. (2013). Paleobathymetry and sequence stratigraphic interpretations from benthic foraminifera: Insights on New Jersey shelf architecture. *IODP Expedition Geosphere*, 313(6), 1488–1513.

SCHMELZ ET AL. 10 of 11



- Kominz, M. A., Browning, J., Miller, K., Sugarman, P., Mizintseva, S., & Scotese, C. (2008). Late Cretaceous to Miocene sea-level estimates from the New Jersey and Delaware coastal plain coreholes: An error analysis. *Basin Research*, 20(2), 211–226.
- Kominz, M. A., Miller, K. G., Browning, J., Katz, M., & Mountain, G. (2016). Miocene relative sea level on the New Jersey shallow continental shelf and coastal plain derived from one-dimensional backstripping: A case for both eustasy and epeirogeny. *Geosphere*, 12(5), 1437–1456.
- Liu, L. (2015). The ups and downs of North America: Evaluating the role of mantle dynamic topography since the Mesozoic. Reviews of Geophysics, 53(3), 1022–1049.
- Lynch-Stieglitz, J., Curry, W. B., & Slowey, N. (1999). A geostrophic transport estimate for the Florida Current from the oxygen isotope composition of benthic foraminifera. *Paleoceanography*, 14(3), 360–373.
- Miller, K. G., Browning, J. V., Schmelz, W. J., Mountain, G. S., Kopp, R. E., & Wright, J. D. (2020a). Cenozoic sea-level and cryospheric evolution from deep-sea geochemical and continental margin records. *Science Advances*, 6(20), eaaz1346.
- Miller, K. G., Kominz, M. A., Browning, J. V., Wright, J. D., Mountain, G. S., Katz, M. E., et al. (2005). The Phanerozoic record of global sea-level change. *Science*, 310(5752), 1293–1298.
- Miller, K. G., Mountain, G. S., Browning, J. V., Kominz, M. A., Sugarman, P. J., Christie-Blick, N., et al. (1998). Cenozoic global sea level, sequences, and the New Jersey transect: Results from coastal plain and continental slope drilling. *Reviews of Geophysics*, 36(4), 569–601.
- Miller, K. G., Mountain, G. S., Wright, J. D., & Browning, J. V. (2011). A 180-million-year record of sea level and ice volume variations from continental margin and deep-sea isotopic records. *Oceanography*, 24(2), 40–53.
- Miller, K. G., Schmelz, W. J., Browning, J. V., Kopp, R. E., Mountain, G. S., & Wright, J. D. (2020b). Ancient sea level as key to the future. Oceanography, 33(2), 32–41.
- Mitrovica, J., Beaumont, C., & Jarvis, G. (1989). Tilting of continental interiors by the dynamical effects of subduction. *Tectonics*, 8(5), 1079–1094
- Moucha, R., Forte, A. M., Mitrovica, J. X., Rowley, D. B., Quéré, S., Simmons, N. A., et al. (2008). Dynamic topography and long-term sea-level variations: There is no such thing as a stable continental platform. *Earth and Planetary Science Letters*, 271(1–4), 101–108.
- Moucha, R., & Ruetenik, G. A. (2017). Interplay between dynamic topography and flexure along the U.S. Atlantic passive margin: Insights from landscape evolution modeling. *Global and Planetary Change*, 149, 72–78.
- Mountain, G., Proust, J. N., McInroy, D., Cotterill, C., & the Expedition 313 Scientists (2010). Proceedings of the International Ocean Drilling Program, Expedition 313, (Vol. 313, pp. U1339–U1345). Tokyo: Integrated Ocean Drilling Program Management International, Inc.. https://doi.org/10.2204/iodp.proc.313.2010
- Müller, R. D., Zahirovic, S., Williams, S. E., Cannon, J., Seton, M., & Bower, D. J., et al. (2019). A global plate model including lithospheric deformation along major rifts and orogens since the Triassic. *Tectonics*, 38(6), 1884–1907.
- Müller, R. D., Sdrolias, M., Gaina, C., Steinberger, B., & Heine, C. (2008). Long-term sea-level fluctuations driven by ocean basin dynamics. Science, 319(5868), 1357–1362.
- Petersen, K. D., Nielsen, S. B., Clausen, O. R., Stephenson, R., & Gerya, T. (2010). Small-Scale mantle convection produces stratigraphic sequences in sedimentary basins. *Science*, 329(5993), 827–830.
- Rasmussen, C. E., & Williams, C. K. (2006). Gaussian processes for machine learning, Cambridge, MA: MIT Press.
- Raymo, M. E., Kozdon, R., Evans, D., Lisiecki, L., & Ford, H. L. (2018). The accuracy of mid-Pliocene δ18O-based ice volume and sea level reconstructions. *Earth-Science Reviews*, 177, 291–302.
- Rowley, D. B., Forte, A. M., Moucha, R., Mitrovica, J. X., Simmons, N. A., & Grand, S. P. (2013). Dynamic topography change of the eastern United States since 3 million years ago. *Science*, 340(6140), 1560–1563.
- Spasojevic, S., & Gurnis, M. (2012). Sea level and vertical motion of continents from dynamic earth models since the Late Cretaceous. AAPG Bulletin. 96(11), 2037–2064.
- Spasojević, S., Liu, L., Gurnis, M., & Müller, R. D. (2008). The case for dynamic subsidence of the U.S. east coast since the Eocene. *Geophysical Research Letters*, 35(8), L08305. 10.1029/2008GL033511
- Van Sickel, W. A., Kominz, M. A., Miller, K. G., & Browning, J. V. (2004). Late Cretaceous and Cenozoic sea-level estimates: Backstripping analysis of borehole data, onshore New Jersey. Basin Research, 16(4), 451–465.
- Watts, A., & Steckler, M. (1979). Subsidence and eustasy at the continental margin of eastern North America. M. Talwani W. Hay & W.B.F. Ryan. *Deep Drilling Results in the Atlantic Ocean: Continental Margins and Paleoenvironment*, Maurice Ewing Series, 3, 218–234). Washington DC: American Geophysical Union. https://doi.org/10.1029/ME003p0218
- Winnick, M. J., & Caves, J. K. (2015). Oxygen isotope mass-balance constraints on Pliocene sea level and East Antarctic Ice Sheet stability. *Geology*, 43(10), 879–882.
- Wright, N. M., Seton, M., Williams, S. E., Whittaker, J. M., & Müller, R. D. (2020). Sea-level fluctuations driven by changes in global ocean basin volume following supercontinent break-up. *Earth-Science Reviews*, 208, 103293.

SCHMELZ ET AL. 11 of 11